Geophysical Research Letters

RESEARCH LETTER
10.1029/2020GL087911

Key Points:
- Tropospheric warming and drying, induced by a regional climate feedback spurred on by the expansion of the Hadley circulation under global warming, enhance and sustain the recent long-term increasing trend in large wildfires in the western United States
- Due to its unique climatology, western United States has the most robust long-term large wildfire increasing trend in North America during 1984–2014
- Warming and drying by adiabatic compression of sinking air, and increased low level offshore, downslope winds play key roles

Supporting Information:
- Supporting Information S1

Correspondence to:
W. Lau,
wkmlau@umd.edu

Citation:
Zhang, L., Lau, W., Tao, W., & Li, Z. (2020). Large wildfires in the western United States exacerbated by tropospheric drying linked to a multi-decadal trend in the expansion of the Hadley circulation. *Geophysical Research Letters*, *47*, e2020GL087911. https://doi.org/10.1029/2020GL087911

Received 15 APR 2020
Accepted 21 JUL 2020
Accepted article online 4 AUG 2020

Large Wildfires in the Western United States Exacerbated by Tropospheric Drying Linked to a Multi-Decadal Trend in the Expansion of the Hadley Circulation

L. Zhang[1], W. Lau[2], W. Tao[2,3], and Z. Li[1,2]

[1]Department of Atmospheric and Oceanic Science, University of Maryland, College Park, MD, USA, [2]Earth System Science Interdisciplinary Center, University of Maryland, College Park, MD, USA, [3]State Key Laboratory of Numerical Modeling for Atmospheric Sciences and Geophysical Fluid Dynamics, Institute of Atmospheric Physics, Chinese Academy of Sciences, Beijing, China

Abstract Analyses of wildfire-climate relationships in North America were conducted using diverse independent observation and reanalysis data sets for the period 1984–2014. Results show that the western United States (WUS) has experienced the most robust increase in burned area, even though Alaska and western-central Canada have comparable warming trends. In addition to warming, the WUS has been under the influence of multi-decadal trends in tropospheric relative humidity deficit, reduced cloudiness, increased surface net insolation, and enhanced adiabatic warming and drying from increased tropospheric subsidence, as well as drying from enhanced offshore low-level flow. These trends are found to be associated with a widening of the descending branch of the Hadley circulation, consistent with climate model projections under greenhouse gases warming. Due to the relative short (~30 years) data record, the aforementioned trend signals are likely also be affected by phase changes of natural interdecadal variability during the data period.

Plain Language Summary The increase in wildfires in the western United States (WUS) has been attributed to numerous factors, such as enhanced warming, drying, and ignitions by humans or nature and possibly amplified by a regional climate feedback. However, the mechanisms of the feedback are not well understood. Our observational analyses show that the increase in wildfires in the WUS is likely linked to a multi-decadal drying trend in the subtropical troposphere associated with the expansion of the Hadley circulation under greenhouse-gas warming. This circulation change induces a regional climate feedback, involving reduced relative humidity, fewer clouds, more downward surface insolation, warmer land surfaces, enhanced subsidence, and stronger offshore low-level winds. This results in accelerated and sustained tropospheric warming and drying, exacerbating wildfires in the WUS. Results suggest that if actions to combat climate change are not taken soon, the WUS wildfire situation will likely worsen quickly.

1. Introduction

Staggering socioeconomic losses stemming from more frequent and severe wildfires in North America (NA) in recent decades have drawn much attention to the need for better understanding the causes of increased wildfires, in order to inform and provide sound strategies for mitigation. Numerous studies have found significant increasing trends in occurrence, total burned area, and duration of wildfires in the western United States (WUS), most pronounced in the forests of the northern U.S. Rocky Mountains (Dennison et al., 2014; Westerling et al., 2006). Burned areas of large fires have doubled in the boreal region of Canada and Alaska from 1959 to 1999 (Kasischke & Turetsky, 2006). These increased wildfire activities have been linked to natural climate variability and human activities (Abatzoglou & Williams, 2016; Balch et al., 2017; Harvey, 2016; Littell et al., 2009). Warmer temperatures, earlier snowing melting, prolonged summer droughts, vegetation type, and increased lightning are believed to be key factors contributing to the frequency, severity, and length of wildfires (Holden et al., 2018; Littell et al., 2016; Running, 2006; Veblen et al., 2000; Veraverbeke et al., 2017; Westerling et al., 2003, 2006). These studies and others have led to the following assessment statement (Wuebbles, 2017): "The incidence of large forest fires in western United States and Alaska has increased since the early 1980 (*high confidence*) and is projected to further increase in those regions as the climate warms with profound change to certain ecosystems (*medium confidence*)."

Contemporaneously, there have also been multiple lines of evidence indicating that greenhouse-gas (GHG)-induced global warming may have increased droughts over the globe during recent decades (Dai et al., 2004; Dai, 2006, 2011; Dai & Zhao, 2017), together with the expansion of semiarid and desert regions (Huang et al., 2016). Such a global drying trend is projected to worsen in the future, mainly due to an increased water vapor deficit (Dai, 2013; Dai et al., 2018; Feng & Fu, 2013; Lau & Kim, 2015; Zhao & Dai, 2017). Recent studies suggest that the impact of anthropogenic climate change on fire weather is emerging above natural variability in NA (Abatzoglou et al., 2019; Kirchmeier-Young et al., 2017). It is important to stress that the trend pattern of burned areas based on the relatively short data record used here (~30 years) could signal not only GHG warming but the effects of natural variability, such as the Interdecadal Pacific Oscillation (IPO; Dong & Dai, 2015). Here, we focus more on the GHG warming effect, based on our previous modeling results. Modeling studies have suggested increased atmospheric dryness, that is, the reduction in relative humidity (RH) and the increased frequency and duration of dry spells in the subtropics and midlatitudes located over the western regions of major continents. These could be a component of a canonical global pattern of precipitation and large-scale circulation in response to GHG-induced warming (Lau et al., 2013). This pattern involves changes in the Hadley circulation (HC), linking a narrowing of the intertropical convergence zone (ITCZ) with enhanced precipitation, to an expanding subtropical subsiding zone with reduced RH in the middle and lower troposphere via the so-called Deep Tropical Squeeze (DTS) radiation-dynamical feedback effect (Lau & Kim, 2015, 2017). The reduction in near-surface RH is important to the occurrence and spread of wildfires because of its close relationship to the water stress on vegetation. Low near-surface RH and high temperatures increase the vapor pressure deficit (VPD), enhance the evaporative demand, and accelerate the drying of vegetation, resulting in increased fire fuel and potential for large and severe wildfires (Holden et al., 2018; Seager et al., 2015; Williams et al., 2014). The physical relationships among wildfires in NA and regional feedback processes to changes in the large-scale circulation, global dryness, and linkages to GHG-induced warming are still poorly understood. In this paper, we aim to provide observational evidence revealing these relationships and shed new light on the underlying regional climate processes affecting wildfire trends in NA and linkages with climate change under GHG warming.

2. Data and Methods

Data analyses were conducted using multiple independent data sets of wildfire and climate control variables in NA for the period 1984–2014, that is, in situ measurements, satellite observations, and five reanalyses products. Burned area information available from the Monitoring Trends in Burn Severity (MTBS) database (Eidenshink et al., 2007) and the Canadian National Fire Database (CNFDB) database were employed. The MTBS maps burned areas across the United States from 1984 to the present, including all fires larger than 1,000 acres in the WUS and 500 acres in the eastern United States. Although large wildfires account for a small portion of the total number of wildfires, these large wildfires contribute toward nearly 95% of the total burned area. In our study, a total of 12,279 large wildfires were examined for the United States. Unlike the MTBS, the CNFDB data set includes all sizes of forest fires. We selected wildfires larger than 500 acres for consistency with the MTBS. A total of 13,614 large fires from the CNFDB were examined. Here, the fire season is defined as running from May to September. All fires labeled as prescribed fires (i.e., man-made fires) were excluded. To facilitate the quantitative analysis, the burned area data were processed into $1° \times 1°$ grid boxes at a monthly temporal resolution.

Concerning climate control variables, we used near-surface RH from the HadISDH global monthly land surface data set ($5° \times 5°$) provided by the Meteorological Office Hadley Centre (Smith et al., 2011; Willett et al., 2014), based on subdaily, quality-controlled data collected from HadISDH stations since 1973. Despite its relatively coarse spatial resolution, it is a unique, in situ observations-only climate-data gridded product that is homogenized and physically consistent. The total cloud amount was obtained from the International Satellite Cloud Climatology Project (ISCCP). The new ISCCP H-series of products extends the period of record to 1982–2014, providing monthly averages of cloud properties at a $1° \times 1°$ spatial resolution (Rossow & Schiffer, 1991). National Aeronautics and Space Administration's (NASA) Surface Radiation Budget data set provided shortwave (SW) radiative fluxes, covering 24 years (1984–2007). This $1° \times 1°$ global gridded product was generated from satellite-derived cloud parameters, reanalysis-based meteorological parameters, and a few other ancillary data sets. For drought estimates, we used National Center for Atmospheric Research's (NCAR) self-calibrated Palmer Drought Severity Index (PDSI) with

Penman-Monteith potential evapotranspiration (Dai et al., 2004) because the traditional PDSI uses only temperature and precipitation, which may overestimate the drying effect of rising temperature. The Climatic Research Unit Timeseries V4.04 data set provided daily temperatures and maximum temperatures (Harris et al., 2020). For the large-scale circulation analysis, we used five reanalysis products, that is, the Modern-Era Retrospective analysis for Research and Applications (Version 2), the NCEP-DOE AMIP-II Reanalysis 2, ERA-Interim, the Japanese 55-year *Reanalysis*, and the 20th Century *Reanalysis* (Compo et al., 2011; Dee et al., 2011; Gelaro et al., 2017; Kanamitsu et al., 2002; Kobayashi et al., 2015; see supporting information Table S1 for more detailed information). The reanalysis data sets were remapped onto a uniform $2.5° \times 2.5°$ grid using bilinear interpolation to calculate the multi-reanalysis ensemble mean. All data can be obtained from the links provided in the acknowledgments section.

The wildfire data sets for NA were first examined to identify regions with pronounced regional trends in wildfires and surface air temperature. Second, the trend patterns of key climate control variables, that is, near-surface RH, cloudiness, net downward surface solar radiation, and PDSI, were constructed and examined for correlations with wildfire in each subregion. Finally, circulation and precipitation features associated with global warming trends over the North Pacific and NA, as well as vertical profiles of temperature, RH, and vertical motions, were examined over each subregion using the ensemble means of the five reanalysis products.

3. Results

3.1. Wildfire Trends in NA

We first examine temporal variations and linear trends of wildfire burned areas and surface temperature (May–September), averaged over the United States, Canada, and NA from 1984 to 2014. The NA time series of burned area (Figure 1a) shows large interannual variations and a strong positive trend. This trend is statistically significant ($p < 0.05$) and was reported by others (Dennison et al., 2014; Picotte et al., 2016). The mean total burned area during the 2010s is more than double that during the 1980s. Examining the United States and Canada separately, the increasing wildfire trend seen in NA is mainly due to the increasing trend seen in the United States. Canada shows considerable interannual variations but no significant long-term trend. However, the United States and Canada show similar warming trends ($+0.3°C\ decade^{-1}$) and variabilities in surface temperature (Figure 1b). On a continental scale, a warmer surface temperature thus appears to be a necessary but not sufficient condition for increased wildfires in NA. To understand the differences between warming and wildfire trends in the United States and Canada, we need to examine the spatial distribution of wildfires and their relationships with the regional and global climate forcing and feedback.

The spatial pattern of the burned area trend in NA during the 1984–2014 fire seasons is highly asymmetric (Figure 1c). Both negative and positive trends are present, and significant signals ($p < 0.05$) are found clustered only in those regions with positive trends. Not found are significant clusters of negative trends. Three regions with strongly increasing burned areas (>50–$100\ km^2\ decade^{-1}$) stand out: the WUS, Alaska (AK), and western-central Canada (WCC). WUS in our study includes the states of Washington, Oregon, northern California, Idaho, and the mountain regions of Arizona and New Mexico. WCC includes the provinces of Alberta, Saskatchewan, and the southern Northwest Territories. Negative but weaker trends ($p > 0.05$) in burned areas are found over the western-central Northwest Territories, Manitoba, and parts of Québec. In the WUS, the burned area shows a robust and steady long-term trend (Figure 1d). By contrast, in AK and WCC, trends are weaker and appear to be affected by episodic occurrences of a few exceptionally large fire events in certain years (Figures 1e and 1f). The asymmetry and highly regionally distributed trend patterns in burned area, as well as different temporal variations among WUS, AK, and WCC, suggest the effect of a large-scale, steady background forcing, that is, overall warming of NA (Figure S1) modulated by regional-scale climate feedback processes.

3.2. Related Trends in Key Climate Control Variables

As discussed previously, a reduction in the near-surface RH will likely lead to increased surface VPD, resulting in accelerated drying of vegetation and the increased potential for wildfires (Holden et al., 2018; Williams et al., 2014). Furthermore, a long-term trend in the tropospheric RH deficit is also likely associated with

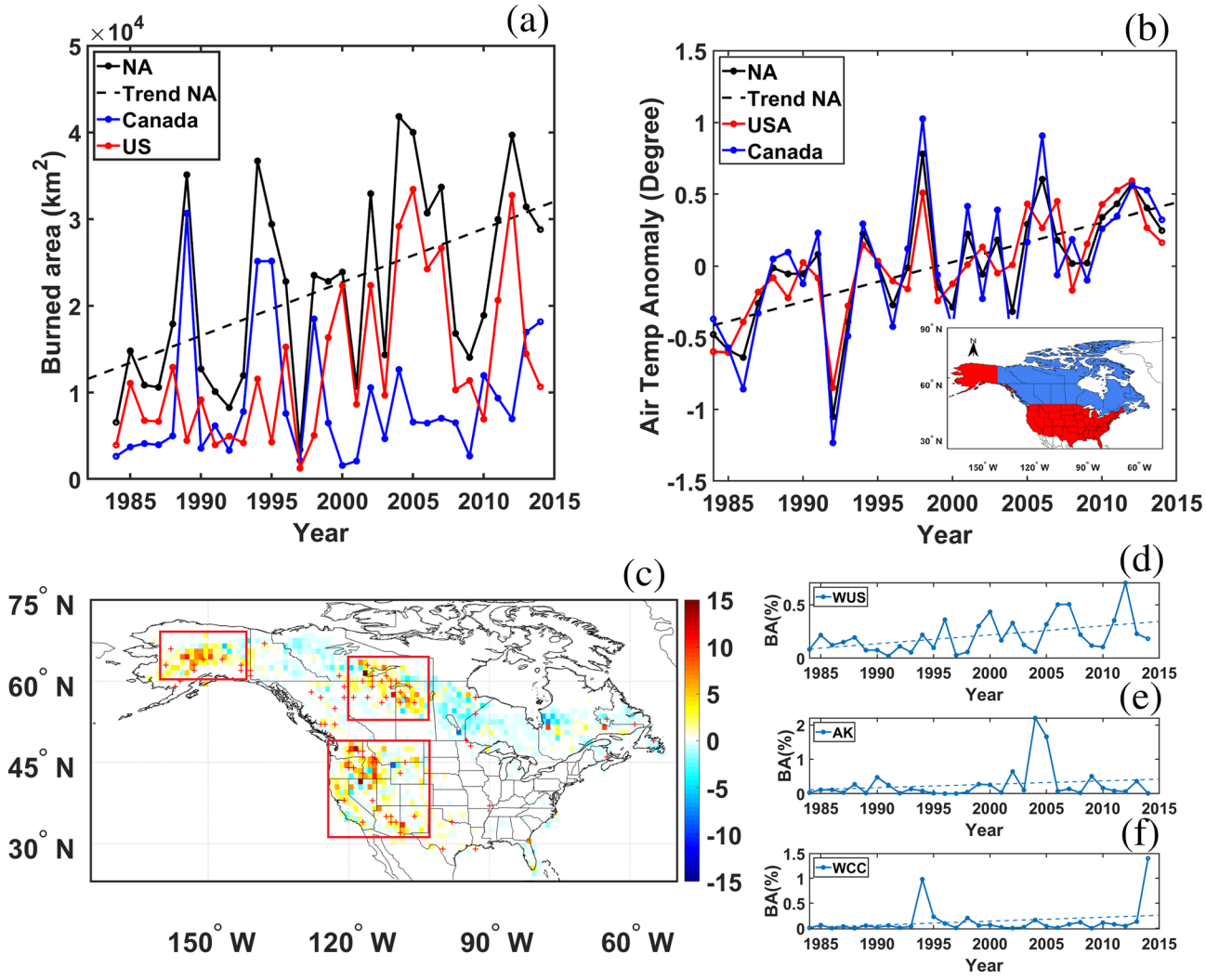

Figure 1. Wildfire and warming trends in North America from 1984–2014 (May–September). Time series of (a) burned area (unit: 10^4 km^2) and (b) surface air temperature anomalies (°C) in North America (black curve), the United States (red curve), and Canada (blue curve). (c) Spatial pattern of linear trends in burned area per 1° × 1° grid box (unit: km^2 decade^{-1}). Statistically significant trends ($p < 0.05$) are denoted by red crosses. (d–f) Time series of burned area percentages with trend lines averaged over domains outlined by the red rectangles in (c), representing (d) the western United States, (e) Alaska, and (f) western central Canada.

suppressed clouds and precipitation. Fewer clouds will lead to reduced SW cloud shielding and enhanced incoming surface SW radiation, leading to sustained warming and drying of the atmosphere-vegetation system and enhanced wildfires. For convenience, we refer to this chain of processes as the regional climate feedback enhancing wildfires (RCFW). In the following, we examine the validity of RCFW in affecting the long-term trend in wildfires in NA by conducting trend and correlation analyses on wildfire burned areas with respect to several key climate control variables, that is, near-surface RH, cloud amount, surface SW downward radiation (SWDR), and PDSI. Figure 2 shows the trend patterns of these climate observables for the wildfire season (May–September). Overall, a north-south dipole pattern in reduced surface RH is found over NA, with strong negative trends (2–3% decade^{-1}) over the southern and WUS and positive trends over the northern Midwest and central Canada (Figure 2a). Over Alaska, the surface RH trend signal is mixed. Figure 2b shows a reduction in total cloud cover over a broad swath spanning Alaska, the Northwest Territories, the Midwest, and eastern United States, with the maximum reduction (10–15% decade^{-1}) occurring over the WUS. The overall reduction in cloudiness is comparable to previous studies showing overall reductions in cloudiness of up to 5% decade^{-1} for the contiguous United States over a

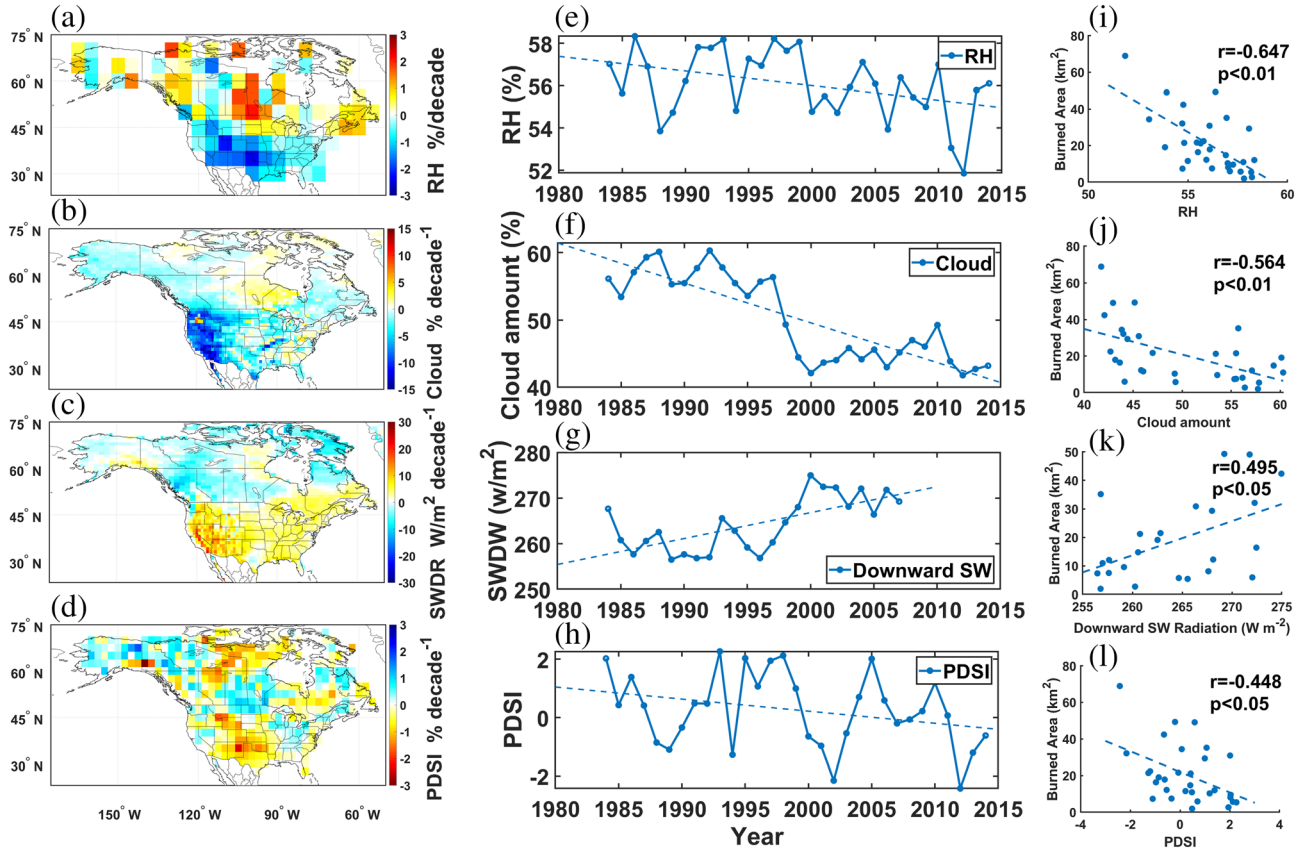

Figure 2. Observed climate changes during 1984–2014 (May–September). Spatial linear trend patterns of (a) near-surface RH (unit: % decade^{-1}), (b) cloud cover (unit: % decade^{-1}), (c) downward SW radiation (W m^{-2} decade^{-1}), and (d) PDSI over North America. Time series of (e) near-surface RH (unit: %), (f) cloud cover (unit: %), (g) surface downward SW radiation (unit: W m^{-2}), and (h) PDSI averaged over the western United States. Panels (i)–(l) show burned area as a function of RH, cloud amount, downward SW radiation, and PDSI, respectively.

similar period (Free et al., 2016; Sun et al., 2015). Increased SWDR is found over the WUS, coinciding with regions of strong cloud and near-surface RH reductions (Figure 2c). Note that SWDR and cloudiness may change in the same way since SWDR is also generated using the ISCCP cloud product. The strong positive SWDR trend over the WUS is consistent with "global brightening" since the mid-1980s (Wild, 2011), attributable in part to reduced cloudiness and aerosols. Based on the PDSI (Figure 2d), a large part of the southern and WUS, central Canada, and parts of southern Alaska are experiencing increased drought conditions (i.e., negative PDSI).

Based on the above results, we computed correlations between burned area and RH, cloud amount, SWDR, and PDSI separately for three key regions showing strong positive trends in burned area (see Figure 1c). During the last three decades, the WUS has experienced decreasing RH (~0.7% decade^{-1}, Figure 2e), decreasing cloud amounts (5.9% decade^{-1}, Figure 2f), increasing SWDR (~5.7 W m^{-2} decade^{-1}) reaching the surface (Figure 2g), and increasing drought severity (negative trend of 0.4% decade^{-1} in PDSI, Figure 2h). Worth noting is that all the aforementioned climate observables show considerable interannual and interdecadal variabilities, linked to natural modes of climate variability, such as the *El Niño-Southern Oscillation*, the Pacific Decadal *Oscillation* (similar to IPO), and the Atlantic Multi-decadal *Oscillation* that could influence fire weather, fuel availability, and ignition (Kitzberger et al., 2007; Pan et al., 2018; Schoennagel et al., 2005; Wang et al., 2014). Taking into account both trends and natural variability, the strongest correlations with burned area are, in descending order, reduced RH (-0.65, $p < 0.01$), cloud amount (-0.56, $p < 0.01$), SWDR ($+0.49$, $p < 0.05$), and PDSI (-0.45, $p < 0.05$), supporting RCFW (Figures 2i–2l). Note that our study period overlaps with a phase change in IPO (Figure S2), switching from a warm phase (1984–1998) to a cold phase (1999–2014). This IPO phase change likely weakened the

"underlying" warming trend during our study period (Dong & Dai, 2015). An additional analysis of the co-variability of the IPO index with RH (detrended) showed mostly weak and insignificant negative correlations (correlation coefficient, $r < 0.3$, $p > 0.05$) over much of NA (see Figure S3). This implies that the surface humidity deficit trend was likely weakened by the negative phase of the IPO during the latter portion of the study period. Examination of the IPO-burned area correlation pattern (Figure S4) shows positive correlations most pronounced over AK, WCC, and the Pacific Northwest. Given the dominance of the cold phase of the IPO during 1999–2014, these positive correlations imply reductions in burned areas, contrary to the underlying increasing trend in burned areas in these regions. This may explain, in part, why the positive trends in burned area are much less pronounced in AK and WCC compared to the WUS (Figures 2d and 2c). In short, the IPO likely confounds the GHG warming signal as represented by the linear trend pattern in our analysis regionally.

Correlation analyses similar to that done for the WUS were carried out for AK and WCC. Table S2 summarizes the results for all three regions. Robust trends in the burned area and significant correlations with all four climate observables are found only in the WUS. For AK, no significant correlations are found in any of the climate observables. For WCC, significant relationships ($p < 0.05$) are found only in RH and PDSI. These suggest that RCFW works for the WUS only but not for AK and WCC. The reasons for these regional differences are explored in the next section.

3.3. Wildfires and GHG Warming

Previous observational and modeling studies have identified features in the large-scale circulation that are likely attributable to GHG warming. These include, among others, multi-decadal trends in strong warming and moistening of the tropical atmosphere (Fu et al., 2011; Lau et al., 2013; Santer et al., 2008, 2016), a rise in the tropical tropopause (Lorenz & DeWeaver, 2007; Seidel & Randel, 2007), a widening of the subtropics and poleward migration of midlatitude storm tracks (Feng & Fu, 2013; Hu & Fu, 2007; Lu et al., 2007; Seidel et al., 2008; Yin, 2005), and the expansion of the global dry lands including the WUS (Dai, 2011; Huang et al., 2016; Seager & Vecchi, 2010). More recently, Coupled Model Intercomparison Project 5 model results have demonstrated that the aforementioned changes are underpinned by the DTS, that is, a structural change in the HC under GHG warming, featuring a narrowing ITCZ core with increased precipitation, linked to increased subsidence and reduced RH in a widening subtropics and poleward shift of the storm tracks (Fu, 2015; Lau & Kim, 2015).

In the following, we examine changes in the large-scale circulation affecting the northeastern Pacific and NA climate using reanalyses data to shed new light on the possible relationship between wildfires in NA and GHG warming. To increase the robustness of the results, we have computed the long-term trend patterns of tropospheric temperature, RH, sea-level pressure (SLP), winds, vertical motion, and precipitation for 1984–2014, based on the ensemble mean of five independent reanalyses. As mentioned previously, the trend signals could be contributed by both GHG effects and multi-decadal natural variability. Here, we only focus on the detection of possible impact on WUS wildfire from a relatively short climate record that could be consistent with changes in the HC attributable to GHG warming, as projected by climate models.

As revealed by the latitude-height cross section of the zonal annual mean temperature trend pattern (Figure 3a), during 1984–2014, a strong warming of the entire troposphere and cooling in the lower stratosphere (above 150 hPa) occurred, a well-recognized signature of global GHG warming (Fu et al., 2011; Santer et al., 2008, 2016). Associated with the tropospheric warming, the annual mean RH trend (Figure 3b) displays a pattern characteristic of increased RH in the deep tropics but strong RH reductions in the tropical upper troposphere. We can see that the descending arms of regions with RH deficits are over the subtropics and midlatitudes of both hemispheres. The RH trend pattern is similar to model projections attributable to global warming (Sherwood et al., 2010). The pattern can be understood in terms of the faster rate of increased saturated vapor pressure with temperature, as governed by the Clausius-Clapeyron law of thermodynamics, compared to the actual increase in ambient vapor pressure due to transport processes (Lau & Kim, 2015; Sherwood et al., 2010). Increased dry advection from above by enhanced anomalous descent in the subtropics and midlatitudes can lead to a further RH deficit in the lower troposphere and near the surface due to the expansion of the HC under GHG warming (Hu & Fu, 2007; Lau & Kim, 2015). In association with the trend in reduced zonal mean RH, an east-west dipole anomalous SLP pattern, with high SLP centers over the North and East Pacific and WUS coupled to low SLP centers over the rest of NA, is established

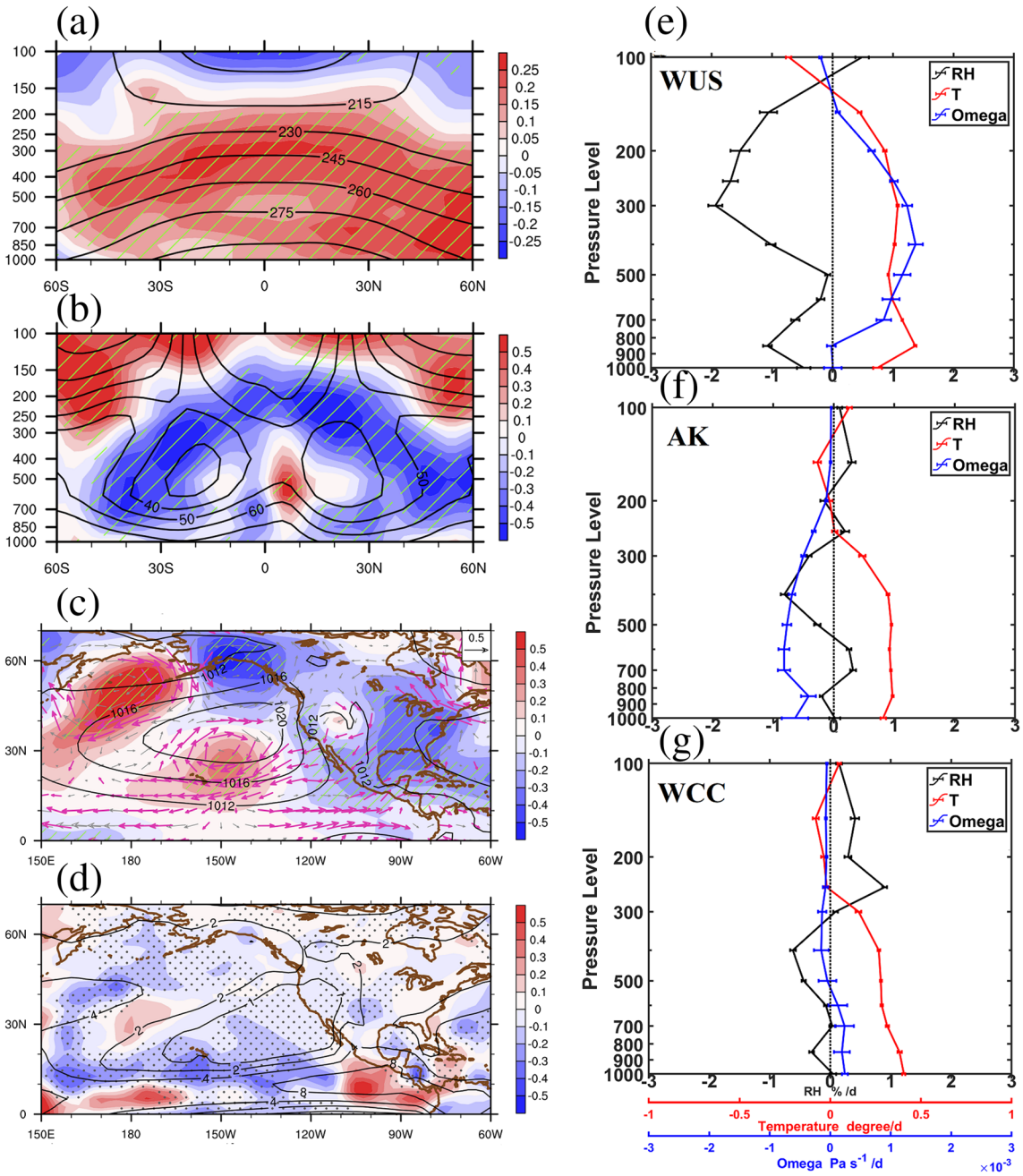

Figure 3. Left panels: Latitude-height cross sections of the linear trends (1984–2014, annual mean) in (a) temperature (unit: °C decade^{-1}) and (b) RH (unit: % decade^{-1}). Spatial patterns of mean linear trends (1984–2014, May–September) in (c) sea-level pressure (unit: hPa decade^{-1}) and 700-hPa winds (arrows, m s^{-1} decade^{-1}), and (d) precipitation (mm day^{-1} decade^{-1}) and 500-hPa vertical motion (Pa s^{-1} decade^{-1}). Trends are shown by color shading, and the contours are the 1984–2014 climatology. Areas with anomalous descending motions are indicated by black dots in (d). Right panels: Vertical profiles of the linear trend (1984–2014, May–September) in temperature (red curve, °C decade^{-1}), RH (black curve, % decade^{-1}), and vertical *p* velocity (blue curve, Pa s^{-1} decade^{-1}), with positive values denoting sinking motion for (e) the western United States, (f) Alaska, and (g) western-central Canada, based on the ensemble mean of five reanalysis data sets. Standard errors of the mean are shown as horizontal error bars.

during the peak wildfire season (May–September). This signals an intensification and expansion of the North Pacific Subtropical High (NPSH, Figure 3c). The eastward extension of the NPSH, signaled by the development of an anomalous high SLP center over the WUS, is likely strongly affected by regional topographic effects. Specifically, an anomalous anticyclonic circulation center is anchored over the elevated arid region of the Great Basin, east of the Rocky Mountains (Figure 3c). As the cold and dry air

masses descend in a clockwise rotation from high elevations to lower valley regions of the coastal mountain ranges, they are heated by adiabatic compression. This would cause a further rapid drop in RH, leading to gusty winds due to air density differences. These hot and dry offshore winds, combined with dry vegetation during summer and fall, would fan more large wildfires. The anomalous SLP center likely intensifies the Santa Ana and Diablo winds (in the fall season), affecting wildfires and prolonging the fire season. Long-term changes in wind gusts affecting wildfires and their relationships with GHG warming are currently subjects of numerous studies and debate (Guzman-Morales & Gershunov, 2019; Hughes et al., 2011; Jin et al., 2015; Miller & Schlegel, 2006; Yue et al., 2014).

Strong trends in suppressed precipitation and widespread anomalous sinking motions at 500 hPa are found over much of the subtropical and midlatitude regions of the Northeast Pacific and NA (Figure 3d). Analysis of time series of vertical motion at 500 hPa over the climatological NPSH region (30–45°N, 140–90°W) and burned area over WUS (Figure S5) shows significant correlation ($r = 0.45$, p value $= 0.011$), indicating a close relationship between WUS wildfire and enhanced subsidence in the descending branch of the HC. Also found is a strong reduction in precipitation along the northern edge of the ITCZ near 10–15°N and increased precipitation near the equator. These features mirror those associated with the DTS under global warming (Lau & Kim, 2015). Note that the WUS is geographically located in a semiarid zone at the eastern edge of the NPSH. It is thus possible that changes in RH, cloudiness, SWDR, precipitation, and circulation arising from the tropical influence due to global warming may affect wildfires in the WUS more strongly than in other regions in NA. This may explain, in part, the lack of strong and coherent signals in burned areas in AC and WCC to our chosen climate control variables. Influences from phase change of IPO could be another important factor that may confound the GHG signal, since the warm phase of IPO tends to cool these two regions and suppress the fire weather condition (Dong & Dai, 2015).

To further explore RCFW's influence on the WUS, we next examine the trend patterns of vertical profiles of RH, vertical p velocity (omega), and temperature from multi-reanalysis data averaged over the WUS (Figure 3e) during the wildfire season (May–September). Most noteworthy is the robust warming trend (0.3–0.5°C decade^{-1}) in the atmospheric column from the surface to 200 hPa. A strong trend in sinking motion (positive omega) is found from 800 to 150 hPa, with a maximum trend (up to 1.5×10^{-3} Pa s^{-1} decade^{-1}) near 400 hPa. As discussed previously, both increased temperature and subsidence can lead to a large RH deficit. The RH profile shows a reduction over the entire atmospheric column, with a maximum decreasing trend (~2% decade^{-1}) at 300 hPa and a secondary maximum (~1% decade^{-1}) near 850–900 hPa. This secondary low-level maximum RH reduction is likely related to the dry advection effect of the enhanced offshore low-level flow, as well as the increased intensity of warmer and drier winds by adiabatic compression, descending from higher elevations inland to coastal areas across the central and southern WUS region (see the discussion for Figure 3c). As shown in Figure 2, the RH deficit is associated with reduced cloud cover and precipitation and increased surface solar radiation, likely enhancing the warming of the Earth's surface. Adiabatic warming of the descending air would also enhance the warming of the atmospheric column, further reducing RH. These feedback processes would thus amplify the GHG warming and the drying of the WUS atmosphere-land system. At the same time, reduced RH leads to increased VPD and enhanced evapotranspiration from leaves, thus accelerating the drying of vegetation and the land surface, promoting more wildfires. Over AK and WCC (Figures 3f and 3g), while the tropospheric warming signal is strong, RH and vertical motion do not show coherent signals in the vertical, indicating a lack of RCFW.

4. Conclusions and Discussion

A comprehensive analysis of long-term wildfire data sets in NA revealed the most significant increasing trend in wildfires in the WUS. A plausible mechanism is put forth, involving regional climate feedbacks enhancing recent wildfire trends as follows. An RH deficit associated with the drying of the subtropics under global warming inhibits convection, suppresses cloudiness and precipitation, and minimizes the SW cloud-shielding effect, resulting in enhanced net downward surface SW radiation. The increased SW radiation at the surface accentuates an already warming land-atmosphere system and, through RCFW, amplifies the RH deficit, increasing the VPD and drying of vegetation and potentially spurring on more severe wildfires. The response in the WUS is likely a regional manifestation of a global drying trend associated with

the expansion of the subsidence branch of the HC, coupled to increased precipitation in the ITCZ in the deep tropics, consistent with model projections of GHG induced (Hu & Fu, 2007; Lau & Kim, 2015). Our results also show that the development of an anomalous high surface pressure center over the Great Basin, associated with the global drying trend and HC changes, may be instrumental in enhancing offshore winds, fanning more large wildfires in the WUS.

The WUS, geographically located in a subtropical semiarid zone along the eastern edge of the NPSH, is more likely subjected to the strong influences of the HC expansion and RCFW. In Alaska and western-central Canada, the other two regions in NA with significant but weaker long-term trends in large wildfire burned areas, RCFW is either weak or absent. We suggest that this may be due to the high-latitude locations of these regions, where tropical influences on wildfires, such as the "Deep Tropical Squeeze," are diminished. The wildfire burned area in these regions may be more impacted by other climate controls, such as storm tracks and jet-stream dynamics, as well as possibly increased lightning ignition and the northward migration of the boreal forest associated with arctic warming (Box et al., 2019; Veraverbeke et al., 2017). It is important to note that the contribution of IPO may have confounded the climate and wildfire trends in our study. The positive correlation with burned area and IPO could be yet another reason for the less robust positive trends in large burned areas in Alaska and Canada compared to the WUS, given the positive-to-negative phase change of the IPO, that is, a cooling tendency of the North Pacific during latter part of our study period. However, separating the influence of GHG warming and multi-decadal internal variability requires a longer data period for burned areas and warrants future investigations. Finally, it remains to be investigated whether RCFW is operative over other continental vegetated land regions (East Asia, Europe, South Africa, Australia, and South America) affected by global warming and atmospheric drying. If so, more wildfires on a global scale are likely to increase emissions of GHG and light-absorbing aerosols, such as black carbon and organic carbon. These can further warm the atmosphere-land surface by absorption of solar radiation and reduction in snow albedo, exacerbating greenhouse warming, thus completing the climate-wildfire feedback loop (Liu et al., 2010, 2014). These are important subjects for future studies.

Data Availability Statement

All data used in this work are available online: Burned area data are available from MTBS (https://www.mtbs.gov/direct-download) and the Canada National Fire Database (https://cwfis.cfs.nrcan.gc.ca/datamart); surface RH observations (https://www.metoffice.gov.uk/hadobs/hadisdh/download420.html); ISCCP cloud data (https://www.ncei.noaa.gov/data/international-satellite-cloud-climate-project-isccp-h-series-data/access/isccp/); surface radiation product from the NASA/GEWEX Surface Radiation Budget project (https://eosweb.larc.nasa.gov/project/srb/srb_table/); PDSI data from NCAR (https://climatedataguide.ucar.edu/climate-data/palmer-drought-severity-index-pdsi); surface temperature data from CRU TS v4 (https://catalogue.ceda.ac.uk/uuid/89e1e34ec3554dc98594a5732622bce9); five reanalysis data sets, including MERRA2 (https://gmao.gsfc.nasa.gov/reanalysis/MERRA-2/data_access/), JRA55 (https://climatedataguide.ucar.edu/climate-data/jra-55), the 20th Century Reanalysis (https://www.psl.noaa.gov/data/20thC_Rean/), NCEP/DOE Reanalysis 2 (R2) Project data sets (https://climatedataguide.ucar.edu/climate-data/ncep-reanalysis-r2), and ERA-Interim data (https://www.ecmwf.int/en/forecasts/datasets/reanalysis-datasets/era-interim).

Acknowledgments
This work is supported by the NASA National Climate Assessment Program (NNH14ZDA001N-INC).

References

Abatzoglou, J. T., & Williams, A. P. (2016). Impact of anthropogenic climate change on wildfire across western US forests. *Proceedings of the National Academy of Sciences USA*, *113*(42), 11,770–11,775. https://doi.org/10.1073/pnas.1607171113

Abatzoglou, J. T., Williams, A. P., & Barbero, R. (2019). Global emergence of anthropogenic climate change in fire weather indices. *Geophysical Research Letters*, *46*, 326–336. https://doi.org/10.1029/2018GL080959

Balch, J. K., Bradley, B. A., Abatzoglou, J. T., Nagy, R. C., Fusco, E. J., & Mahood, A. L. (2017). Human-started wildfires expand the fire niche across the United States. *Proceedings of the National Academy of Sciences USA*, *114*(11), 2946–2951. https://doi.org/10.1073/pnas.1617394114

Box, J. E., Colgan, W. T., Christensen, T. R., Schmidt, N. M., Lund, M., Parmentier, F. J. W., et al. (2019). Key indicators of Arctic climate change: 1971–2017. *Environmental Research Letters*, *14*(4), 045010. https://doi.org/10.1088/1748-9326/aafc1b

Compo, G. P., Whitaker, J. S., Sardeshmukh, P. D., Matsui, N., Allan, R. J., Yin, X., et al. (2011). The twentieth century reanalysis project. *Quarterly Journal of the Royal Meteorological Society*, *137*(654), 1–28. https://doi.org/10.1002/qj.776

Dai, A. (2006). Recent climatology, variability, and trends in global surface humidity. *Journal of Climate*, *19*(15), 3589–3606. https://doi.org/10.1175/JCLI3816.1

Dai, A. (2011). Drought under global warming: A review. *Wiley Interdisciplinary Reviews: Climate Change*, *2*(1), 45–65. https://doi.org/10.1002/wcc.81

Dai, A. (2013). Increasing drought under global warming in observations and models. *Nature Climate Change*, *3*, 52–58. https://doi.org/10.1038/nclimate1633

Dai, A., Trenberth, K. E., & Qian, T. (2004). A global dataset of palmer drought severity index for 1870–2002: Relationship with soil moisture and effects of surface warming. *Journal of Hydrometeorology*, *5*(6), 1117–1130. https://doi.org/10.1175/JHM-386

Dai, A., & Zhao, T. (2017). Uncertainties in historical changes and future projections of drought. Part I: Estimates of historical drought changes. *Climatic Change*, *144*, 519–533. https://doi.org/10.1007/s10584-016-1705-2

Dai, A., Zhao, T., & Chen, J. (2018). Climate change and drought: A precipitation and evaporation perspective. *Current Climate Change Reports*, *4*(3), 301–312. https://doi.org/10.1007/s40641-018-0101-6

Dee, D. P., Uppala, S. M., Simmons, A. J., Berrisford, P., Poli, P., Kobayashi, S., et al. (2011). The ERA-interim reanalysis: Configuration and performance of the data assimilation system. *Quarterly Journal of the Royal Meteorological Society*, *137*(656), 553–597. https://doi.org/10.1002/qj.828

Dennison, P. E., Brewer, S. C., Arnold, J. D., & Moritz, M. A. (2014). Large wildfire trends in the western United States, 1984–2011. *Geophysical Research Letters*, *41*, 2928–2933. https://doi.org/10.1002/2014GL059576

Dong, B., & Dai, A. (2015). The influence of the interdecadal Pacific oscillation on temperature and precipitation over the globe. *Climate Dynamics*, *45*(9–10), 2667–2681. https://doi.org/10.1007/s00382-015-2500-x

Eidenshink, J. C., Schwind, B., Brewer, K., Zhu, Z.-L., Quayle, B., & Howard, S. M. (2007). A project for monitoring trends in burn severity. *Fire Ecology*, *3*(1), 321. https://doi.org/10.4996/fireecology.0301003

Feng, S., & Fu, Q. (2013). Expansion of global drylands under a warming climate. *Atmospheric Chemistry and Physics*, *13*(19), 10,081–10,094. https://doi.org/10.5194/acp-13-10081-2013

Free, M., Sun, B., & Yoo, H. L. (2016). Comparison between total cloud cover in four reanalysis products and cloud measured by visual observations at U.S. weather stations. *Journal of Climate*, *29*(6), 2015–2021. https://doi.org/10.1175/JCLI-D-15-0637.1

Fu, Q., Manabe, S., & Johanson, C. M. (2011). On the warming in the tropical upper troposphere: Models versus observations. *Geophysical Research Letters*, *38*, L15704. https://doi.org/10.1029/2011GL048101

Fu, R. (2015). Global warming-accelerated drying in the tropics. *Proceedings of the National Academy of Sciences USA*, *112*(12), 3593–3594. https://doi.org/10.1073/pnas.1503231112

Gelaro, R., McCarty, W., Suárez, M. J., Todling, R., Molod, A., Takacs, L., et al. (2017). The modern-era retrospective analysis for research and applications, version 2 (MERRA-2). *Journal of Climate*, *30*(Iss 13), 5419–5454. https://doi.org/10.1175/JCLI-D-16-0758.1

Guzman-Morales, J., & Gershunov, A. (2019). Climate change suppresses Santa Ana winds of southern California and sharpens their seasonality. *Geophysical Research Letters*, *46*, 2772–2780. https://doi.org/10.1029/2018GL080261

Harris, I., Osborn, T. J., Jones, P., & Lister, D. (2020). Version 4 of the CRU TS monthly high-resolution gridded multivariate climate dataset. *Scientific data*, *7*, 109. https://doi.org/10.1038/s41597-020-0453-3

Harvey, B. J. (2016). Human-caused climate change is now a key driver of forest fire activity in the western United States. *Proceedings of the National Academy of Sciences USA*, *113*(42), 11,649–11,650. https://doi.org/10.1073/pnas.1612926113

Holden, Z. A., Swanson, A., Luce, C. H., Jolly, W. M., Maneta, M., Oyler, J. W., et al. (2018). Decreasing fire season precipitation increased recent western US forest wildfire activity. *Proceedings of the National Academy of Sciences USA*, *115*(36), E8349–E8357. https://doi.org/10.1073/pnas.1802316115

Hu, Y., & Fu, Q. (2007). Observed poleward expansion of the Hadley circulation since 1979. *Atmospheric Chemistry and Physics*, *7*(19), 5229–5236. https://doi.org/10.5194/acp-7-5229-2007

Huang, J., Ji, M., Xie, Y., Wang, S., He, Y., & Ran, J. (2016). Global semi-arid climate change over last 60 years. *Climate Dynamics*, *46*(3), 1131–1150. https://doi.org/10.1007/s00382-015-2636-8

Hughes, M., Hall, A., & Kim, J. (2011). Human-induced changes in wind, temperature and relative humidity during Santa Ana events. *Climatic Change*, *109*(1), 119–132. https://doi.org/10.1007/s10584-011-0300-9

Jin, Y., Goulden, M. L., Faivre, N., Veraverbeke, S., Sun, F., Hall, A., et al. (2015). Identification of two distinct fire regimes in Southern California: Implications for economic impact and future change. *Environmental Research Letters*, *10*(9), 094005. https://doi.org/10.1088/1748-9326/10/9/094005

Kanamitsu, M., Ebisuzaki, W., Woollen, J., Yang, S.-K., Hnilo, J. J., Fiorino, M., & Potter, G. L. (2002). NCEP–DOE AMIP-II reanalysis (R-2). *Bulletin of the American Meteorological Society*, *83*(11), 1631–1644. https://doi.org/10.1175/BAMS-83-11-1631

Kasischke, E. S., & Turetsky, M. R. (2006). Recent changes in the fire regime across the North American boreal region—Spatial and temporal patterns of burning across Canada and Alaska. *Geophysical Research Letters*, *33*, L09703. https://doi.org/10.1029/2006GL025677

Kirchmeier-Young, M. C., Zwiers, F. W., Gillett, N. P., & Cannon, A. J. (2017). Attributing extreme fire risk in Western Canada to human emissions. *Climatic Change*, *144*(2), 365–379. https://doi.org/10.1007/s10584-017-2030-0

Kitzberger, T., Brown, P. M., Heyerdahl, E. K., Swetnam, T. W., & Veblen, T. T. (2007). Contingent Pacific–Atlantic Ocean influence on multicentury wildfire synchrony over western North America. *Proceedings of the National Academy of Sciences USA*, *104*(2), 543–548. https://doi.org/10.1073/pnas.0606078104

Kobayashi, S., Ota, Y., Harada, Y., Ebita, A., Moriya, M., Onoda, H., et al. (2015). The JRA-55 reanalysis: General specifications and basic characteristics. *Journal of the Meteorological Society of Japan. Ser. II*, *93*(1), 5–48. https://doi.org/10.2151/jmsj.2015-001

Lau, W. K. M., & Kim, K.-M. (2015). Robust Hadley circulation changes and increasing global dryness due to CO_2 warming from CMIP5 model projections. *Proceedings of the National Academy of Sciences USA*, *112*(12), 3630–3635, 201418682. https://doi.org/10.1073/pnas.1418682112

Lau, W. K. M., & Kim, K.-M. (2017). Competing influences of greenhouse warming and aerosols on Asian summer monsoon circulation and rainfall. *Asia-Pacific Journal of Atmospheric Sciences*, *53*(Iss 2), 181–194. https://doi.org/10.1007/s13143-017-0033-4

Lau, W. K. M., Wu, H.-T., & Kim, K.-M. (2013). A canonical response of precipitation characteristics to global warming from CMIP5 models. *Geophysical Research Letters*, *40*, 3163–3169. https://doi.org/10.1002/grl.50420

Littell, J. S., McKenzie, D., Peterson, D. L., & Westerling, A. L. (2009). Climate and wildfire area burned in western U.S. ecoprovinces, 1916–2003. *Ecological Applications*, *19*(4), 1003–1021. https://doi.org/10.1890/07-1183.1

Littell, J. S., Peterson, D. L., Riley, K. L., Liu, Y., & Luce, C. H. (2016). A review of the relationships between drought and forest fire in the United States. *Global Change Biology*, *22*(7), 2353–2369. https://doi.org/10.1111/gcb.13275

Liu, Y., Goodrick, S., & Heilman, W. (2014). Wildland fire emissions, carbon, and climate: Wildfire–climate interactions. *Forest Ecology and Management*, *317*, 80–96. https://doi.org/10.1016/j.foreco.2013.02.020

Liu, Y., Stanturf, J., & Goodrick, S. (2010). Trends in global wildfire potential in a changing climate. *Forest Ecology and Management*, *259*(4), 685–697. https://doi.org/10.1016/j.foreco.2009.09.002

Lorenz, D. J., & DeWeaver, E. T. (2007). Tropopause height and zonal wind response to global warming in the IPCC scenario integrations. *Journal of Geophysical Research*, *112*, D10119. https://doi.org/10.1029/2006JD008087

Lu, J., Vecchi, G. A., & Reichler, T. (2007). Expansion of the Hadley cell under global warming. *Geophysical Research Letters*, *34*, L06805. https://doi.org/10.1029/2006GL028443

Miller, N. L., & Schlegel, N. J. (2006). Climate change projected fire weather sensitivity: California Santa Ana wind occurrence. *Geophysical Research Letters*, *33*, L15711. https://doi.org/10.1029/2006GL025808

Pan, X., Chin, M., Ichoku, C. M., & Field, R. D. (2018). Connecting Indonesian fires and drought with the type of El Niño and phase of the Indian Ocean dipole during 1979–2016. *Journal of Geophysical Research: Atmospheres*, *123*, 7974–7988. https://doi.org/10.1029/2018JD028402

Picotte, J. J., Peterson, B. E., Meier, G., & Howard, S. M. (2016). 1984–2010 trends in fire burn severity and area for the conterminous US. *International Journal of Wildland Fire*, *25*(4), 413–420. https://doi.org/10.1071/WF15039

Rossow, W. B., & Schiffer, R. A. (1991). ISCCP cloud data products. *Bulletin of the American Meteorological Society*, *72*(1), 2–20. https://doi.org/10.1175/1520-0477(1991)072<0002:ICDP>2.0.CO;2

Running, S. W. (2006). Climate change: Is global warming causing more, larger wildfires? *Science*, *313*(5789), 927–928. https://doi.org/10.1126/science.1130370

Santer, B. D., Thorne, P. W., Haimberger, L., Taylor, K. E., Wigley, T. M. L., Lanzante, J. R., et al. (2008). Consistency of modelled and observed temperature trends in the tropical troposphere. *International Journal of Climatology*, *28*(13), 1703–1722. https://doi.org/10.1002/joc.1756

Santer, B. D., Solomon, S., Pallotta, G., Mears, C., Po-Chedley, S., Fu, Q., & Bonfils, C. (2016). Comparing tropospheric warming in climate models and satellite data. *Journal of Climate*, *30*(1), 373–392. https://doi.org/10.1175/JCLI-D-16-0333.1

Schoennagel, T., Veblen, T. T., Romme, W. H., Sibold, J. S., & Cook, E. R. (2005). ENSO and PDO variability affect drought-induced fire occurrence in Rocky Mountain subalpine forests. *Ecological Applications*, *15*(6), 2000–2014. https://doi.org/10.1890/04-1579

Seager, R., Hooks, A., Williams, A. P., Cook, B., Nakamura, J., & Henderson, N. (2015). Climatology, variability, and trends in the US vapor pressure deficit, an important fire-related meteorological quantity. *Journal of Applied Meteorology and Climatology*, *54*(6), 1121–1141. https://doi.org/10.1175/JAMC-D-14-0321.1

Seager, R., & Vecchi, G. A. (2010). Greenhouse warming and the 21st century hydroclimate of southwestern North America. *Proceedings of the National Academy of Sciences USA*, *107*(50), 21,277–21,282. https://doi.org/10.1073/pnas.0910856107

Seidel, D. J., Fu, Q., Randel, W. J., & Reichler, T. J. (2008). Widening of the tropical belt in a changing climate. *Nature Geoscience*, *1*(1), 21–24. https://doi.org/10.1038/ngeo.2007.38

Seidel, D. J., & Randel, W. J. (2007). Recent widening of the tropical belt: Evidence from tropopause observations. *Journal of Geophysical Research*, *112*, D20113. https://doi.org/10.1029/2007JD008861

Sherwood, S. C., Ingram, W., Tsushima, Y., Satoh, M., Roberts, M., Vidale, P. L., & O'Gorman, P. A. (2010). Relative humidity changes in a warmer climate. *Journal of Geophysical Research*, *115*, D09104. https://doi.org/10.1029/2009JD012585

Smith, A., Lott, N., & Vose, R. (2011). The integrated surface database: Recent developments and partnerships. *Bulletin of the American Meteorological Society*, *92*(6), 704–708. https://doi.org/10.1175/2011BAMS3015.1

Sun, B., Free, M., Yoo, H. L., Foster, M. J., Heidinger, A., & Karlsson, K.-G. (2015). Variability and trends in U.S. cloud cover: ISCCP, PATMOS-x, and CLARA-A1 compared to homogeneity-adjusted weather observations. *Journal of Climate*, *28*(11), 4373–4389. https://doi.org/10.1175/JCLI-D-14-00805.1

Veblen, T. T., Kitzberger, T., & Donnegan, J. (2000). Climatic and human influences on fire regimes in ponderosa pine forests in the Colorado Front Range. *Ecological Applications*, *10*(4), 1178–1195. https://doi.org/10.1890/1051-0761(2000)010[1178:CAHIOF]2.0.CO;2

Veraverbeke, S., Rogers, B. M., Goulden, M. L., Jandt, R. R., Miller, C. E., Wiggins, E. B., & Randerson, J. T. (2017). Lightning as a major driver of recent large fire years in North American boreal forests. *Nature Climate Change*, *7*(7), 529–534. https://doi.org/10.1038/nclimate3329

Wang, S., Huang, J., He, Y., & Guan, Y. (2014). Combined effects of the Pacific decadal oscillation and El Niño-southern oscillation on global land dry-wet changes. *Scientific Reports*, *4*, 6651. https://doi.org/10.1038/srep06651

Westerling, A. L., Gershunov, A., Brown, T. J., Cayan, D. R., & Dettinger, M. D. (2003). Climate and wildfire in the western United States. *Bulletin of the American Meteorological Society*, *84*(5), 595–604. https://doi.org/10.1175/BAMS-84-5-595

Westerling, A. L., Hidalgo, H. G., Cayan, D. R., & Swetnam, T. W. (2006). Warming and earlier spring increase western U.S. forest wildfire activity. *Science*, *313*(5789), 940–943. https://doi.org/10.1126/science.1128834

Wild, M. (2011). Enlightening global dimming and brightening. *Bulletin of the American Meteorological Society*, *93*(1), 27–37. https://doi.org/10.1175/BAMS-D-11-00074.1

Willett, K. M., Dunn, R. J. H., Thorne, P. W., Bell, S., de Podesta, M., Parker, D. E., et al. (2014). HadISDH land surface multi-variable humidity and temperature record for climate monitoring. *Climate of the Past*, *10*(6), 1983–2006. https://doi.org/10.5194/cp-10-1983-2014

Williams, A. P., Seager, R., Berkelhammer, M., Macalady, A. K., Crimmins, M. A., Swetnam, T. W., et al. (2014). Causes and implications of extreme atmospheric moisture demand during the record-breaking 2011 wildfire season in the southwestern United States. *Journal of Applied Meteorology and Climatology*, *53*(12), 2671–2684. https://doi.org/10.1175/JAMC-D-14-0053.1

Wuebbles, D. (2017). Climate science special report: fourth national climate assessment (NCA4), volume I|GlobalChange.gov. Retrieved September 25, 2019, from https://www.globalchange.gov/browse/reports/climate-science-special-report-fourth-national-climate-assessment-nca4-volume-i

Yin, J. H. (2005). A consistent poleward shift of the storm tracks in simulations of 21st century climate. *Geophysical Research Letters*, *32*, L18701. https://doi.org/10.1029/2005GL023684

Yue, X., Mickley, L. J., & Logan, J. A. (2014). Projection of wildfire activity in southern California in the mid-twenty-first century. *Climate Dynamics*, *43*(7-8), 1973–1991. https://doi.org/10.1007/s00382-013-2022-3

Zhao, T., & Dai, A. (2017). Uncertainties in historical changes and future projections of drought. Part II: Model-simulated historical and future drought changes. *Climatic Change*, *144*(3), 535–548. https://doi.org/10.1007/s10584-016-1742-x